Quasi Steady-State Model for Power System Stability: Limitations, Analysis and a Remedy

Xiaozhe Wang, Hsiao-Dong Chiang
Cornell University
Ithaca, NY 14850, USA
xw264@cornell.edu, hc63@cornell.edu

Abstract—The quasi steady-state (QSS) model tries to reach a good compromise between accuracy and efficiency in long-term stability analysis. However, the QSS model is unable to provide correct approximations and stability assessment for the long-term stability model consistently. In this paper, some numerical examples in which the QSS model was stable while the long-term stability model underwent instabilities are presented with analysis in nonlinear system framework. At the same time, a hybrid model which serves as a remedy to the QSS model is proposed according to causes for failure of the QSS model and dynamic mechanisms of long-term instabilities. Numerical examples are given to show that the developed hybrid model can successfully capture unstable behaviors of the long-term stability model while the QSS model fails.

Index Terms—quasi steady-state model, long-term stability model, hybrid model, nonlinear analysis, power system long-term stability.

I. Introduction

THE long-term stability model in power system is large and involves different time scales, thus its time domain simulation is expensive in terms of computational efforts and data processing. The quasi steady-state (QSS) model proposed in [1] [2] seeks to reach a good compromise between accuracy and efficiency. By assuming that fast variables are infinitely fast and are stable in the long term, the QSS model replaces the differential equations of short-term dynamics by their equilibrium equations.

The assumptions behind the QSS model that the post-fault system is stable in short-term period and the QSS model is singularity-free are not necessarily satisfied. These issues of the QSS model were addressed in [3]- [5]. Nevertheless, even when these assumptions are satisfied, the QSS model can still provide incorrect approximations for the long-term stability model while little attention was paid to this severe problem before [6]. Some examples were presented in [6] [7] to illustrate limitations of the QSS model with nonlinear analysis. In addition, a theoretical foundation for the QSS model was proposed in [8] where sufficient conditions of the QSS model for accurate approximation of the long-term

Xiaozhe Wang is with the Department of Electrical and Computer Engineering, Cornell University, Ithaca, NY 14850, USA. E-mail: xw264@cornell.edu. Phone: 607-592-4050.

Hsiao-Dong Chiang is with the Department of Electrical and Computer Engineering, Cornell University, Ithaca, NY 14850, USA. Email: hc63@cornell.edu. Phone: 607-255-5270.

stability model in terms of trajectories and ω-limit set were derived.

In this paper, we show that the QSS model can miss two kinds of long-term instabilities. Some numerical examples in which the QSS model was stable while the long-term stability model underwent instabilities are presented. At the same time, nonlinear analysis and some dynamic mechanisms behind failure of the QSS model are given. In addition, a hybrid model which serves as a remedy to the QSS model is proposed, and numerical examples show that the hybrid model can capture unstable behaviors of the long-term stability model while the QSS model fails.

This paper is organized as follows. Section II briefly reviews power system models and their formulations in nonlinear system framework. Section III presents two examples to illustrate limitations of the QSS model followed by some general dynamic mechanisms of long-term instabilities. A hybrid model is proposed in Section IV with numerical schemes. Then Section V gives two numerical examples to show that the hybrid model can capture unstable behaviors of the long-term stability model while the QSS model fails. Conclusions as well as perspectives are stated in Section VI.

II. Power System Models

The long-term stability model for calculating system dynamic response relative to a disturbance can be described as:

$$\dot{z}_c = \epsilon h_c(z_c, z_d, x, y) \quad (1)$$
$$z_d(k) = h_d(z_c, z_d(k-1), x, y) \quad (2)$$
$$\dot{x} = f(z_c, z_d, x, y) \quad (3)$$
$$0 = g(z_c, z_d, x, y) \quad (4)$$

Equation (4) describes the transmission system and the internal static behaviors of passive devices, and (3) describes the internal dynamics of devices such as generators, their associated control systems, certain loads, and other dynamically modeled components. Equations (1) and (2) describe long-term dynamics including exponential recovery load, turbine governor, load tap changer (LTC), over excitation limiter (OXL), etc. f, g and z_c are continuous functions and h_d are discrete functions. Vector x, y are short-term state variables and algebraic variables; z_c, z_d are continuous and discrete long-term state variables respectively. Besides, $1/\epsilon$ is the maximum time constant among devices. Note that shunt compensation switching and LTC operation are typical discrete events

captured by (2), in which case z_d are shunt susceptance and transformer ratio correspondingly. Transitions of z_d depend on system variables, thus z_d change values from $z_d(k-1)$ to $z_d(k)$ at distinct times t_k where $k = 1, 2, 3, ...N$, otherwise, these variables remain constants. Since short-term dynamics have much smaller time constants compared with those of long-term dynamics, x are termed as fast state variables while z_c and z_d are termed as slow state variables.

A. Models in Nonlinear System Framework

If we represent the long-term stability model and the QSS model in τ time scale, where $\tau = t\epsilon$, and denote $\prime$ as $\frac{d}{d\tau}$, then the long-term stability model of power system can be represented as:

$$
\begin{aligned}
z_c' &= h_c(z_c, z_d, x, y), & z_c(\tau_0) = z_{c0} \quad (5)\\
z_d(k) &= h_d(z_c, z_d(k-1), x, y), & z_d(\tau_0) = z_d(0) \quad (6)\\
\epsilon x' &= f(z_c, z_d, x, y), & x(\tau_0) = x_0^l \quad (7)\\
0 &= g(z_c, z_d, x, y) & (8)
\end{aligned}
$$

At the same time, the QSS model can be represented as:

$$
\begin{aligned}
z_c' &= h_c(z_c, z_d, x, y), & z_c(\tau_0) = z_{c0} \quad (9)\\
z_d(k) &= h_d(z_c, z_d(k-1), x, y), & z_d(\tau_0) = z_d(0) (10)\\
0 &= f(z_c, z_d, x, y) & (11)\\
0 &= g(z_c, z_d, x, y) & (12)
\end{aligned}
$$

As stated before, the discrete variables only jump at distinct times while remain constants otherwise in power system models. Thus whenever discrete variables jump in the long-term stability model, z_d update firstly according to (6), and then the long-term stability model moves according to Eqn (5) (7) (8) with z_d fixed as parameters. Similarly, when (10) works in the QSS model, discrete variables update firstly according to (10), and then the QSS model evolves as Eqn (9) (11) (12) with z_d fixed as parameters.

In this paper, we assume that the sequence of control governed by (6) and (10) are the same in the long-term stability model and the QSS model. In other words, control sequences including shunt compensation switching, LTC changing and load shedding are the same in both models.

If we are interested in the study region $U = D_{z_c} \times D_{z_d} \times D_x \times D_y$, where $D_{z_c} \subseteq \Re^p$, $D_{z_d} \subseteq \Re^q$, $D_x \subseteq \Re^m$, $D_y \subseteq \Re^n$, then we have the following facts:
Fact 1.(Locations of Equilibrium Points) Both models have the same set of equilibrium points $E = \{(z_c, z_d, x, y) \in U : z_d(k) = z_d(k-1), h_c(z_c, z_d, x, y) = 0, f(z_c, z_d, x, y) = 0, g(z_c, z_d, x, y) = 0\}$.

Furthermore, assuming $(z_{cls}, z_{dls}, x_{ls}, y_{ls}) \in E$, and let $\phi_l(\tau, z_{c0}, z_d(0), x_0^l, y_0^l)$ denote trajectory of the long-term stability model with initial condition $(z_{c0}, z_d(0), x_0^l, y_0^l)$ and $\phi_q(\tau, z_{c0}, z_d(0), x_0^q, y_0^q)$ denote trajectory of QSS model with initial condition $(z_{c0}, z_d(0), x_0^q, y_0^q)$, then the stability region of the long-term stability model is:

$$
A_l(z_{cls}, z_{dls}, x_{ls}, y_{ls}) := \{(z_c, z_d, x, y) \in U : \phi_l(\tau, z_{c0}, \\
z_d(0), x_0^l, y_0^l) \to (z_{cls}, z_{dls}, x_{ls}, y_{ls}) \text{ as } \tau \to +\infty\} \quad (13)
$$

And the stability region of the QSS model is:

$$
A_q(z_{cls}, z_{dls}, x_{ls}, y_{ls}) := \{(z_c, z_d, x, y) \in \Gamma : \phi_q(\tau, z_{c0}, \\
z_d(0), x_0^q, y_0^q) \to (z_{cls}, z_{dls}, x_{ls}, y_{ls}) \text{ as } \tau \to +\infty\} \quad (14)
$$

where $\Gamma := \{(z_c, z_d, x, y) \in U : f(z_c, z_d, x, y) = 0, g(z_c, z_d, x, y) = 0\}$ is the constraint manifold of the QSS model.

The singular points of constraint manifold Γ are:

$$
S := \{(z_c, z_d, x, y) \in \Gamma : \det \begin{bmatrix} D_x f & D_y f \\ D_x g & D_y g \end{bmatrix} = 0\} \quad (15)
$$

For each fixed $z_c \in D_{z_c}$ and $z_d(k) \in D_{z_d}$, given a point $(z_c, z_d(k), x, y)$ on Γ, the corresponding transient stability model is defined as:

$$
\begin{aligned}
\dot{x} &= f(z_c, z_d(k), x, y) \quad (16)\\
0 &= g(z_c, z_d(k), x, y)
\end{aligned}
$$

If $(z_c, z_d(k), x, y) \notin S$, then by Implicit Function Theorem, there exists a unique solution $(z_c, z_d(k), l(z_c, z_d(k)))$ locally near the point $(z_c, z_d(k), x, y)$ such that:

$$
\begin{aligned}
f(z_c, z_d(k), l(z_c, z_d(k))) &= 0 \quad (17)\\
g(z_c, z_d(k), l(z_c, z_d(k))) &= 0
\end{aligned}
$$

where

$$
\begin{pmatrix} x_{ts} \\ y_{ts} \end{pmatrix} = \begin{pmatrix} l_1(z_c, z_d(k)) \\ l_2(z_c, z_d(k)) \end{pmatrix} = l(z_c, z_d(k))
$$

$(z_c, z_d(k), x_{ts}, y_{ts})$ is termed as an equilibrium point of the transient stability model. If $(z_c, z_d(k), x_{ts}, y_{ts})$ is a stable equilibrium point (SEP) of the transient stability model, then the stability region of $(z_c, z_d(k), x_{ts}, y_{ts})$ is represented as:

$$
A_t(z_c, z_d(k), x_{ts}, y_{ts}) := \{(x, y) \in D_x \times D_y : \phi_t(t, z_c, \\
z_d(k), x, y) \to (z_c, z_d(k), x_{ts}, y_{ts}) \text{ as } t \to +\infty\} \\
(18)
$$

where $\phi_t(t, z_c, z_d(k), x, y)$ denotes the trajectory of the transient stability model (16).

Assuming that $D_y g$ is nonsingular, then transient stability model (16) can be linearized near the equilibrium point as:

$$
\dot{x} = (D_x f - D_y f D_y g^{-1} D_x g)x \quad (19)
$$

and we can define the stable component Γ_s of constraint manifold:

$$
\Gamma_s = \{(z_c, z_d, x, y) \in \Gamma : \text{all eigenvalues } \lambda \text{ of} \\
(D_x f - D_y f D_y g^{-1} D_x g) \text{ satisfy Re}(\lambda) < 0, \\
\text{and } D_y g \text{ is nonsingular}\} \quad (20)
$$

such that each point on Γ_s is a SEP of the corresponding transient stability model defined in Eqn (16) for fixed z_c and $z_d(k)$. A comprehensive theory of stability regions can be found in [9]- [15].

III. LIMITATIONS OF THE QSS MODEL

In this section, we firstly present two examples of the QSS model in which the QSS model failed to capture dynamics of the long-term stability model. Then some general physical mechanisms of long-term instabilities are elaborated.

A. Numerical Examples

To best of our knowledge, there are two kinds of instabilities that the QSS model fails to capture in long-term stability analysis. In the first case, the QSS model fails to detect oscillation problems in the long-term stability model as shown in Fig. 1. In this 14-bus system, the system maintained stability in the short-term period when lines between Bus 11-10, Bus 7-9 and Bus 6-11 broke down. The final oscillations were brought by dynamics of OXL. When the LTC between Bus 4 and Bus 9 stopped changing as LTC ratio reached the lower limit, the OXL of generator at Bus 2 reached its limit leading to oscillations of field current i_f and state variable v_{oxl} which further resulted in oscillations of variables of automatic voltage regulators (AVR). As a result, the system had both voltage and electromechanical oscillation problems. However, the QSS model failed to capture the oscillations that happened in the long-term stability model.
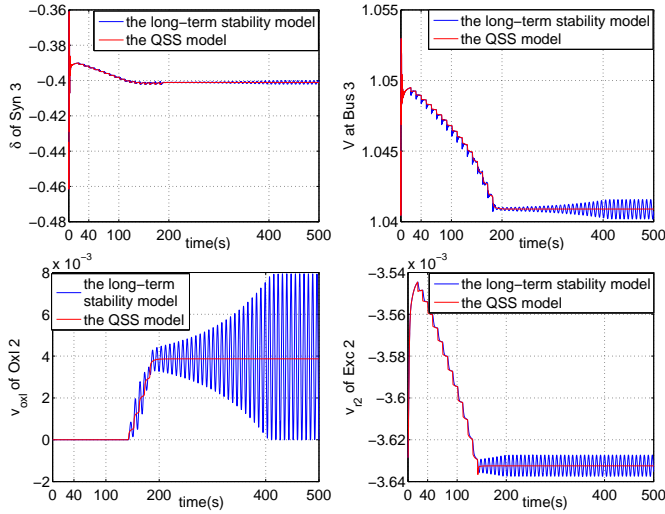

Fig. 1. The trajectory comparisons of the long-term stability model and the QSS model. The QSS model converged to a long-term SEP while the long-term stability model suffered from voltage and electromechanical oscillation problems.

In the second case, the QSS model fails to capture the long-term instability caused by short-term variables as shown in Fig. 2. In this 14-bus system, the system maintained stability in the short-term period when lines between Bus 6-13, Bus 7-9 and Bus 6-11 broke down. The long-term instability was due to the counter effect between LTC and OXL. The OXL of the generator at Bus 2 reached its limit when LTC at Bus 2-4, Bus 4-9 and Bus 12-13 jumped the second time at 40s, however, LTC continued lowering tap ratio afterwards and the counter effect between the LTC and OXL became even severer, which resulted in wild oscillations of variables of AVR. Finally, long-term instability took place. Also, the QSS model didn't provide correct approximations for the long-term stability model with incorrect stability assessment.

The causes for failure of the QSS model were analyzed in nonlinear system framework [6] [7]. From the viewpoint of nonlinear system theories, the cause for failure of the QSS model in both examples here was that the first point
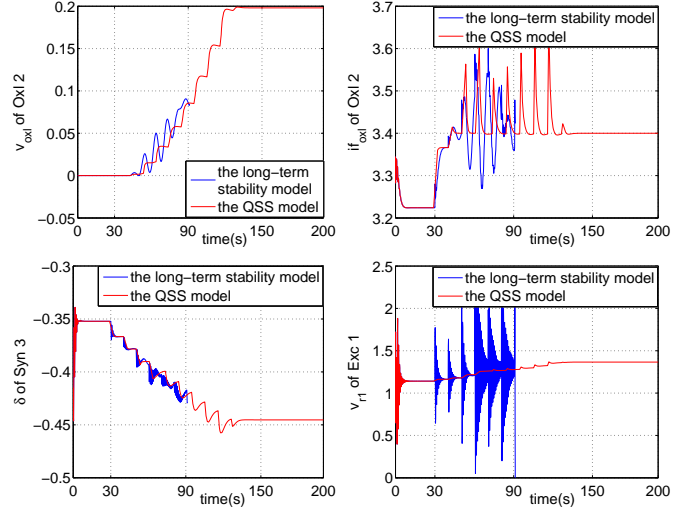

Fig. 2. The trajectory comparisons of the long-term stability model and the QSS model. The QSS model converged to a long-term SEP while the long-term stability model stopped at 101.2155s s due to instabilities caused by wild oscillations of short-term variables.

$(z_{ck}^l, z_d(k), x_k^l, y_k^l)$ on $\phi_l(\tau, z_{c0}, z_d(0), x_0^l, y_0^l)$ after discrete variables jump to $z_d(k)$ lied outside of the stability region $A_t(z_{ck}^q, z_d(k), x_k^q, y_k^q)$ of the corresponding transient stability model, thus slow manifolds of the QSS model and the long-term stability model got separated afterwards and the QSS model could no longer provide correct approximations for the long-term stability model as shown in Fig. 3. Specifically, in the first case, the long-term stability model and the QSS model had different ω-limit sets. The ω-limit set of the QSS model was a stable equilibrium point around which was a limit cycle that the long-term stability converged to. Refer to [6]- [8] for more details.
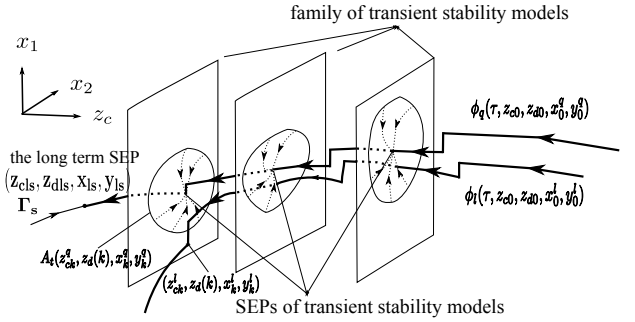

Fig. 3. $(z_{ck}^l, z_d(k), x_k^l, y_k^l)$ on $\phi_l(\tau, z_{c0}, z_d(0), x_0^l, y_0^l)$ lies outside $A_t(z_{ck}^q, z_d(k), x_k^q, y_k^q)$, thus the QSS model can no longer provide correct approximations afterwards.

From these two examples, we can see that when the QSS model failed to capture unstable behaviors of the long-term stability model, OXL were excited. Next, some dynamic mechanisms of long-term instability are going to be elaborated, which further illustrate the important role that OXL plays.

B. Some Dynamic Mechanisms of Long-Term Instabilities

For long-term stability analysis, it's assumed that the system has survived the short-term period after the contingency,

and the study period may extend to several minutes. The long-term instability usually happens in a system which is operating with many lines heavily loaded and reactive power reserves at minimum. The contingency results in an increased reactive power loss on the transmission line and voltage drops consequently at some buses. Assuming the system maintains its stability in short-term time scale by control of AVR and power system stabilizers (PSS) at generators. Then after a time delay, LTC start to work and try to recover load-side voltage by lowering tap ratios, however, LTC may impose an even heavier reactive demand on the generator until OXL of generators are activated. With fewer generators on voltage control, the power system is much prone to voltage instability [16].

The long-term instability is usually classified into two cases, namely long-term voltage instability and instability of short-term dynamics caused by long-term dynamics [1] [17]. Let's firstly consider the long-term voltage instability. This instability may be due to loss of long-term equilibrium when loads try to restore their power beyond the capability of the transmission network and connected generation. Mathematically, that means there is no solution for system (1)-(4) anymore. Besides, the instability may also because post-fault long-term equilibrium point is disturbance unstable [18]. Additionally, dynamic mechanisms of voltage collapse in long-term were explained in [19] [20] in terms of stability regions. It was shown that voltage stability region shrinks as the generator terminal voltage decreases. As a result, when OXL are activated as LTC evolve, the trajectory is easier to leave the shrinking stability region, then voltage collapse takes place.

As for the other case, the evolution of long-term dynamics leads to the instability of short-term variables in the form of sudden transitions. The outcomes include loss of synchronism of field current limited generators, induction motors stalling [17] and electromechanical together with voltage oscillations. One physical mechanism is that the activation of OXL caused by LTC operation leads to wild change of fast variables of AVR and PSS, thus results in instabilities of short-term variables. The examples presented in the last section belong to this kind of instability.

In the next section, a hybrid model is presented as a remedy to the QSS model according to nonlinear analysis of causes for failure of the QSS model as well as physical mechanisms of long-term instabilities.

IV. REMEDY: HYBRID MODEL

From the viewpoint of physical mechanisms, the dynamics of OXL and its counter effect between LTC and load restoration are main causes for long-term instabilities as mentioned in extensive literature [1] [16] [18]- [21]. From the aspect of nonlinear system analysis, when the QSS model fails to provide correct approximations, slow manifolds of the long-term stability model and the QSS model get separated, which is caused mainly by slow dynamics of OXL and LTC. Hence, the deviation of slow variables of OXL between the long-term stability model and the QSS model can be regarded as criteria to judge whether the QSS model works properly. And this is the starting point to develop the hybrid model.

The hybrid model is presented as follows. The QSS model starts to implement after short-term dynamics settle down before which the long-term stability model is used; whenever discrete variables jump, check the distance of variables of OXL of the long-term stability model and that of the QSS model to judge whether the QSS model works properly; when discrete variables stop changing, check whether variables of OXL are positively damped in the long-term stability model to guarantee that there is no oscillation in the long-term stability model. The hybrid model is shown as below.

Hybrid Model

A Run the long-term stability model till τ_1 when short-term dynamics settle down.

B Run the QSS model from τ_1. Whenever discrete variables jump, check whether the distance of variables of OXL of the long-term stability model and that of the QSS model is bigger than threshold η. If yes, switch back to the long-term stability model; Otherwise, continue with the QSS model.

C When all discrete variables stop jumping, check whether variables of OXL are positively damped in the long-term stability model. If yes, the long-term stability model converges to the stable equilibrium point that the QSS model converges to; Otherwise, switch back to the long-term stability model.

Short-term dynamics usually settle down by 20s after the contingency, thus τ_1 was set to be 20s in examples of this paper. On the other hand, η is system-dependent and was set to be 10^{-3} in examples of the paper. In addition, although slow variables $z^l_{\{oxl\}k}$ of OXL on the trajectory of the long-term stability model is needed at **B**, $z^l_{\{oxl\}k}$ can be approximated from trajectory of the QSS model without simulation of the long-term stability model, which are to be discussed more in the next subsection. Also, reinitialization when switching back to the long-term stability model is also to be explained.

A. numerical schemes

Let's firstly consider **B**. Assuming the point on $\phi_q(\tau, z_{c0}, z_d(0), x_0, y_0)$ before discrete variables jump the kth time is $(\bar{z}^q_{c(k-1)}, z_d(k-1), \bar{x}^q_{(k-1)}, \bar{y}^q_{(k-1)})$, if the QSS model works properly before the jump of discrete variables, then the trajectory of the long-term stability model should keep a small distance to $(\bar{z}^q_{c(k-1)}, z_d(k-1), \bar{x}^q_{(k-1)}, \bar{y}^q_{(k-1)})$, thus we approximate the point on the trajectory of the long-term stability model immediately after discrete variables change by a one-step integration in the long-term stability model, i.e.

$$
\begin{aligned}
z'_c &= h_c(z_c, z_d(k), x, y), & z_c(\tau_0) &= \bar{z}^q_{c(k-1)} \quad (21) \\
\epsilon x' &= f(z_c, z_d(k), x, y), & x(\tau_0) &= \bar{x}^q_{(k-1)} \\
0 &= g(z_c, z_d(k), x, y)
\end{aligned}
$$

and denote the approximated point as $(z^l_{ck}, z_d(k), x^l_k, y^l_k)$ with $z^l_{\{oxl\}k} \subset z^l_{ck}$. In addition, assuming the QSS model jumps to $(z^q_{ck}, z_d(k), x^q_k, y^q_k)$ and $z^q_{\{oxl\}k} \subset z^q_{ck}$. If the distance between $z^l_{\{oxl\}k}$ and $z^q_{\{oxl\}k}$ is bigger than threshold η, then switch back to the long-term stability model.

As for **C**, when discrete variables stop jumping, we firstly check whether all generators are working under current limits which means OXL are not excited. If yes, then the long-term stability model converges to the same point that the QSS model converges to; otherwise, suppose the QSS model converges to $(z_{cN}^q, z_d(N), x_N^q, y_N^q)$, then we run the long-term stability model starting from $(z_{cN}^q, z_d(N), x_N^q, y_N^q)$ for several steps, i.e.

$$
\begin{aligned}
z_c' &= h_c(z_c, z_d(N), x, y), & z_c(\tau_0) &= z_{cN}^q \quad (22) \\
\epsilon x' &= f(z_c, z_d(N), x, y), & x(\tau_0) &= x_N^q \\
0 &= g(z_c, z_d(N), x, y)
\end{aligned}
$$

and see whether the magnitude of $z_{\{oxl\}k}$ is decreasing, i.e. $z_{\{oxl\}k}$ is positively damped. If yes, the long-term stability model converges to the same long-term stable equilibrium point as the QSS model; otherwise, the long-term stability model suffers from oscillation problems and we need to switch back to the long-term stability model.

When switching back to the long-term stability model is needed in either **B** or **C**, we need reinitialization for the long-term stability model, i.e. we need to provide initial point for the long-term stability model. For this purpose, we record the point $(z_{c0}, z_d(0), x_{0s}, y_{0s})$ when the QSS model starts to work and each point $(\bar{z}_{c(k-1)}^q, z_d(k-1), \bar{x}_{(k-1)}^q, \bar{y}_{(k-1)}^q)$ on $\phi_q(\tau, z_{c0}, z_d(0), x_0, y_0)$ before discrete variables jump the kth time as the hybrid model runs. Suppose we need to switch back to the long-term stability model when discrete variables jump the kth time, if k is no more than 2, we switch back to the long-term stability model with initial point $(z_{c0}, z_d(0), x_{0s}, y_{0s})$; if k is bigger than 2, we switch back to the long-term stability model with initial point $(\bar{z}_{c(k-3)}^q, z_d(k-3), \bar{x}_{(k-3)}^q, \bar{y}_{(k-3)}^q)$. The block diagram of the hybrid model is shown in Fig. 4.

At the end of this section, we would like to discuss the efficiency of the proposed hybrid model. As you may notice, **B** doesn't require extra computational efforts if the QSS model is implemented without switching back to the long-term stability model. Although **C** requires additional integration during the simulation, the time required is a mere fraction of total time consumed if not neglectable. For instance, to simulate a 14-bus system which was long-term stable up to 300s, the QSS model took 9.50s while the hybrid model took 9.80s, and the long-term stability model required 42.18s. All models used fixed time step for comparison purpose.

V. NUMERICAL ILLUSTRATION

In this section, two examples which are shown in Section III are presented with comparisons with the hybrid model. In the first example, the QSS model failed to capture the oscillation problems caused by OXL. In the second example, the QSS model failed to capture the instability caused by fast variables of AVR. However, in both cases, the hybrid model successfully detected problems of the QSS model and switched back to the long-term stability model, thus provided correct stability assessment. All simulations were done using PSAT 2.1.6 [22].
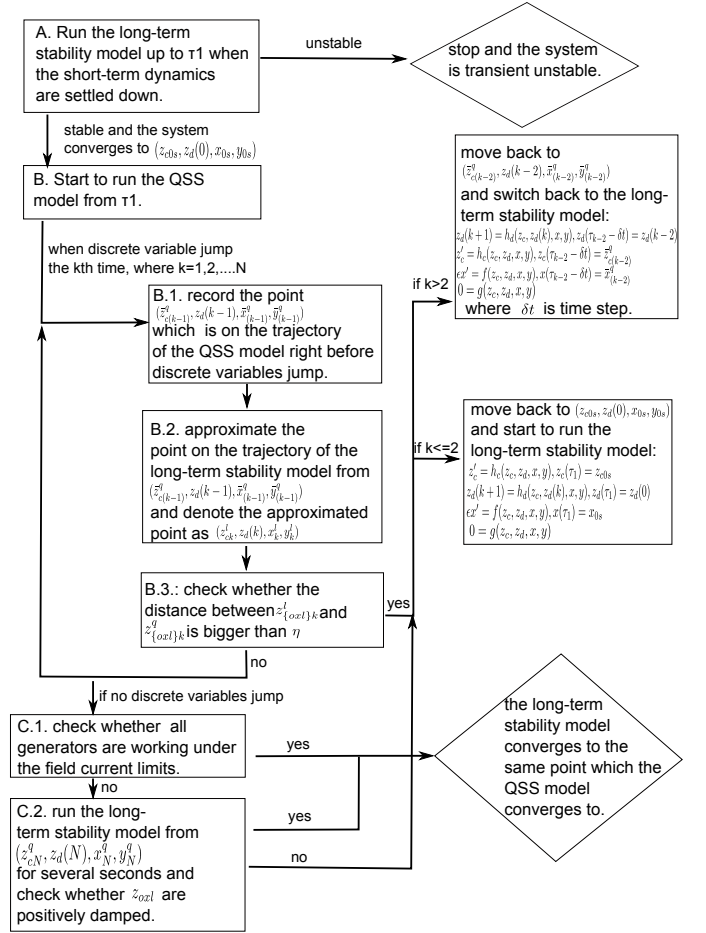

Fig. 4. The block diagram of the hybrid model.

A. Numerical Example I

The first example was the 14-bus system shown in Fig. 1. Each of the five generator was controlled by AVR and OXL whose initial time delay was 40s. Generator 1 and Generator 3 were also controlled by turbine governors. Besides, there were three exponential recovery loads at Bus 9, Bus 10 and Bus 14 respectively. Additionally, there was one LTC between Bus 4 and Bus 9 which had an initial time delay of 20s and fixed tapping delay of 10s. At 1s, there were three line losses including Bus 11-Bus 10, Bus 7-Bus 9, Bus 6-Bus 11. The QSS model started to implement at 20s.

The trajectory comparisons of the long-term stability model, the hybrid model and the QSS model are shown in Fig. 5. The long-term stability model suffered from both voltage and electromechanical oscillation problems brought by OXL dynamics. When the LTC stopped working after 180s, field currents of both the generator at Bus 2 and the generator at Bus 3 reached OXL's limits, and slow variables of OXL were not positive damped since their magnitudes of oscillation were increasing. Finally the long-term stability model converged to a limit cycle around the long-term SEP that the QSS model converged to. However, the QSS model failed to capture oscillation problems in the long-term stability model and provided incorrect stability assessment. On the other hand, the hybrid model detected that there were oscillations in the long-

term stability model, thus it moved back to 160s at which the long-term stability model was implemented. Although there was a difference between the trajectory of the hybrid model and the long-term stability model due to different initial points at 160s, the hybrid model provided correct stability assessment that the system had oscillation problems.

hybrid model successfully captured the unstable behaviors and provided correct stability assessment.
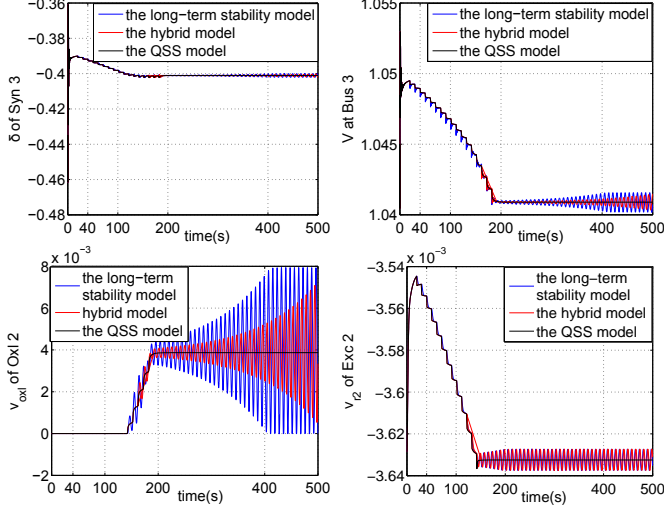

Fig. 5. The trajectory comparisons of the long-term stability model, hybrid model and the QSS model. The hybrid model captured the oscillation problems of the long-term stability model while the QSS model failed.
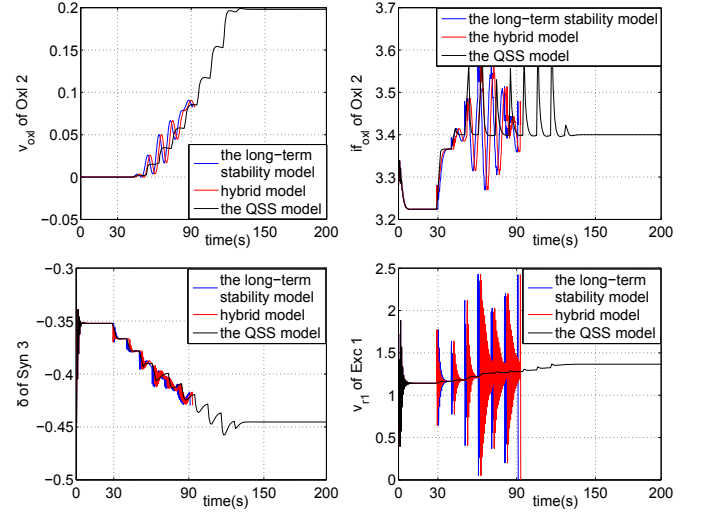

Fig. 6. The trajectory comparisons of the long-term stability model, the hybrid model and the QSS model. The hybrid model successfully captured the instability of the long-term stability model while the QSS model failed.

B. Numerical Example II

This example was the 14-bus system shown in Fig. 2. Each generator was controlled by AVR and OXL whose initial time delay was 30s. Generator 1 and Generator 3 were also controlled by turbine governors. Besides, there were three exponential recovery loads at Bus 9, Bus 10 and Bus 14 respectively. Additionally, there were three LTC between Bus 4 and Bus 9, Bus 12 and 13, Bus 2 and Bus 4. All LTC had initial time delay of 30s and fixed tapping delay of 10s. At 1s, there were three line losses including Bus 6-Bus 13, Bus 7-Bus 9, Bus 6-Bus 11. The QSS model started to implement at 20s.

The trajectory comparisons of the long-term stability model, the hybrid model and the QSS model are shown in Fig. 6. As stated before, OXL of the generator at Bus 2 reached its limit when LTC jumped the second time at 40s. However, LTC continued lowering tap ratio afterwards such that fast variables of AVR were excited and oscillated wildly. The instability of short-term variables finally resulted in long-term instability of the whole system. However, the QSS model failed to capture the unstable behaviors and converged to a long-term SEP, thus provided incorrect stability assessment in concluding that the system was long-term stable. On the other hand, the hybrid model detected that the distance between z_{oxl} of the long-term stability model and that of the QSS model got bigger than the threshold 10^{-3} at 30s, thus the hybrid model moved back to 20s and started to run the long-term stability model with initial condition $(z_{c0}, z_d(0), x_{0s}, y_{0s})$. Hence, the

VI. CONCLUSION

In this paper, two examples in which the QSS model was stable while the long-term stability model underwent instabilities are presented, showing that the QSS model can miss two kinds of long-term instabilities. Causes for failure of the QSS model in nonlinear system framework and some general dynamic mechanisms of long-term instabilities are elaborated, from which we see the important role OXL plays in long-term stability. In addition, a hybrid model which serves as a remedy to the QSS model is proposed with efficient numerical schemes. Finally, numerical examples are given to show that the hybrid model can capture unstable behaviors of the long-term stability model while the QSS model fails.

The proposed hybrid model is based on nonlinear analysis for the QSS model and dynamic mechanisms of long-term instabilities. We would like to provide a theoretical foundation for the hybrid model in the near future.

VII. ACKNOWLEDGMENT

REFERENCES

[1] T. V. Cutsem, *Voltage Stability of Electric Power Systems*. Boston/London/Dordrecht: Kluwer Academic Publishers, 1998.
[2] T. V. Cutsem, Y. Jacquemart, J. N. Marquet, *A Comprehensive Analysis of Mid-term Voltage Stability*. IEEE Transactions on Power Systems, Vol. 10, No. 3, pp. 1173-1182, August 1995.
[3] T. V. Cutsem, M. E. Grenier, D. Lefebvre, *Combined Detailed and Quasi Steady-State Time Simulations for Large-disturbance Analysis*. International Journal of Electrical Power and Energy Systems, Vol. 28, Issue 9, pp. 634-642, November 2006.
[4] P. Rousseaux, T. V. Cutsem *Quasi Steady-State Simulation Diagnosis Using Newton Method with Optimal Multiplier*. IEEE Power Engineering Society General Meeting, 2006.

[5] Q. Wang, H. Song, V. Ajjarapu *Continuation-Based Quasi-Steady-State Analysis*. IEEE Transactions on Power Systems, Vol. 21, No. 1, February 2006.

[6] X. Z. Wang, H. D. Chiang, *Some issues with Quasi-Steady State Model in Long-term Stability* IEEE PES general meeting 2013.

[7] X. Z. Wang, H. D. Chiang, *Numerical Investigations on Quasi Steady-State Model for Voltage Stability: Limitations and Nonlinear Analysis*. submitted to International Transactions on Electrical Energy Systems.

[8] X. Z. Wang, H. D. Chiang, *Analytical Studies of Quasi Steady-State Model in Power System Long-term Stability Analysis*. to appear in IEEE Transactions on Circuits and Systems I: Regular Papers. DOI 10.1109/TCSI.2013.2284171.

[9] H. D. Chiang, *Direct Methods for Stability Analysis of Electric Power Systems-Theoretical Foundation, BCU Methodologies, and Applications*. New Jersey: John Wiley & Sons, Inc, 2011.

[10] H. D. Chiang, M. W. Hirsch, and F. F. Wu, *Stability regions of nonlinear autonomous dynamical systems*. IEEE Transactions on Automatic Control, Vol. 33, No. 1, pp. 16-27, January 1988.

[11] H. D. Chiang, J. S. Thorp, *Stability regions of nonlinear dynamical systems: A constructive methodology*. IEEE Transactions on Automatic Control, Vol. 34, No. 12, pp. 1229-1241, December 1989.

[12] Luis F. C. Alberto, H. D. Chiang, *Theoretical Foundation of CUEP Method for Two-Time Scale Power System Models*. IEEE Power and Energy Society General Meeting, 2009.

[13] V. Veukatasubramanian, H. Schattler and J. Zaborszky, *Dynamics of Large Constrained Nonlinear Systems—A Taxonomy Theory* Proc. IEEE, Vol. 83, pp. 1530-1561, November 1995.

[14] H. Khalil, *Nonlinear System, 3rd ed*, New York: Macmillan Publishing Company, 2002.

[15] J. Zaborszky, G. Huang, B. Zheng, and T. C. Leung, *On the phase portrait of a class of large nonlinear dynamic systems such as the power system*. IEEE Trans. on Automatic Control , Vol. 33, No. 1, pp. 4-15, January 1988.

[16] L. L. Grigsby, ed. *Power system stability and control*. CRC press, 2012.

[17] M. J. Hossain, H. R. Pota, V. Ugrinovskii, *Short and Long-term Dynamic Voltage Instability*. Proceedings of the 17th world congress. Seoul, Korea; July 2008. pp. 9392-9397.

[18] P. Kundur, J. Paserba, V. Ajjarapu, G. Andersson, A. Bose, C. Canizares, N. Hatziargyriou, D. Hill, A. Stankovic, C. Taylor, T. Van Cutsem, V. Vittal, *Definition and Classification of Power System Stability*. IEEE Transactions on Power Systems, Vol. 19, No. 2, pp. 1387-1401, May 2004.

[19] K. T. Vu, C. C. Liu, C. W. Taylor, K. M. Jimma, *Voltage Instability: Mechanisms and Control Strategies* Proceedings of the IEEE, Vol. 83, No. 11, pp. 1442-1455, 1995.

[20] K. T. Vu, C.C. Liu, *Dynamic mechanisms of voltage collapse* Systems & control letters, Vol. 15, No. 4, pp. 329-338, 1990.

[21] S. G. Johansson. *Mitigation of voltage collapse caused by armature current protection*. IEEE Transactions on Power Systems, Vol. 14, No. 2, pp. 591-599,1999.

[22] F. Milano *Power System Analysis Toolbox Documentation for PSAT version 2.1.5, November 1, 2009*.